FACETS
a multidisciplinary open access science journal

RESEARCH ARTICLE

Post-transcriptional regulation of frog innate immunity: discovery of frog microRNAs associated with antiviral responses and ranavirus infection using a *Xenopus laevis* skin epithelial-like cell line

Lauren A. Todd[a], Maxwell P. Bui-Marinos[a], and Barbara A. Katzenback[a]*

[a]Department of Biology, Faculty of Science, University of Waterloo, 200 University Avenue West, Waterloo, ON N2L 3G1 Canada

*barb.katzenback@uwaterloo.ca

OPEN ACCESS

Citation: Todd LA, Bui-Marinos MP, and Katzenback BA. 2021. Post-transcriptional regulation of frog innate immunity: discovery of frog microRNAs associated with antiviral responses and ranavirus infection using a *Xenopus laevis* skin epithelial-like cell line. FACETS 6: 2058–2083. doi:10.1139/facets-2021-0090

Handling Editor: David Lesbarrères

Received: June 30, 2021

Accepted: September 15, 2021

Published: December 16, 2021

Published by: Canadian Science Publishing

Abstract

Post-transcriptional regulators such as microRNAs are emerging as conserved regulators of innate antiviral immunity in vertebrates, yet their roles in amphibian antiviral responses remain uncharacterized. We profiled changes in microRNA expressions in the *Xenopus laevis* skin epithelial-like cell line Xela DS2 in response to poly(I:C)—an analogue of viral double-stranded RNA and inducer of type I interferons—or frog virus 3 (FV3), an immunoevasive virus associated with amphibian mortality events. Small RNA libraries generated from untreated, poly(I:C)-treated, and FV3-infected cells were sequenced. We detected 136 known *X. laevis* microRNAs and discovered 133 novel *X. laevis* microRNAs. Sixty-five microRNAs were differentially expressed in response to poly(I:C), many of which were predicted to target regulators of antiviral pathways such as cGAS-STING, RIG-I/MDA-5, TLR signaling, and type I interferon signaling, as well as products of these pathways (NF-κB-induced and interferon-stimulated genes). In contrast, only 49 microRNAs were altered by FV3 infection, fewer of which were predicted to interact with antiviral pathways. Interestingly, poly(I:C) treatment or FV3 infection downregulated transcripts encoding factors of the host microRNA biogenesis pathway. Our study is the first to suggest that host microRNAs regulate innate antiviral immunity in frogs and sheds light on microRNA-mediated mechanisms of immunoevasion by FV3.

Key words: frog virus 3, microRNAs, antiviral immunity, poly(I:C), skin epithelial cells, *Xenopus laevis*

Introduction

Post-transcriptional mechanisms are emerging as key regulators of immune signaling in vertebrates, and microRNAs (miRNAs) are a prime example of such a mechanism (Boosani and Agrawal 2016). miRNAs are a class of small noncoding RNAs that function in post-transcriptional regulation of gene expression. miRNA genes are transcribed in the nucleus by RNA polymerase II and are processed into hairpin precursors (pre-miRNAs) by the RNase III enzyme Drosha (Lee et al. 2002). Pre-miRNAs are exported to the cytoplasm where they are further processed into mature miRNA duplexes by the RNase III enzyme Dicer (Lee et al. 2002). One strand of the miRNA duplex is degraded, while the

other guides the Argonaute-containing RNA-induced silencing complex to mRNAs which are complementary to the miRNA guide (Lee et al. 2002). Direct interactions between the miRNA and mRNA (typically the 3′ untranslated region (UTR)) induce degradation or inhibit translation of the mRNA (Lee et al. 2002).

Vertebrate miRNAs have been found to regulate the expression of genes involved in antiviral signaling pathways that produce interferons (IFNs) and inflammatory cytokines in response to pathogen infection (Boosani and Agrawal 2016). Host miRNAs have been shown to regulate components of key pathogen sensing pathways such as the cytosolic RIG-I/MDA5 sensing pathway (Li et al. 2020), endosomal TLR3 pathway (Tili et al. 2007; Hou et al. 2009; Imaizumi et al. 2010), endosomal/cell surface TLR4 pathway (Wendlandt et al. 2012), and endosomal TLR7/8/9 pathways (Hou et al. 2009; Tang et al. 2009), as well as the JAK-STAT signaling pathway that regulates the production of IFN-stimulated genes (ISGs) (Tang et al. 2009; Jarret et al. 2016). In some cases, these interactions promote efficient host immune responses. However, viral infection can induce changes in host miRNA expression that detriment the host. For example, Coxsackievirus B3-induced miR-30a suppresses TRIM25 and RIG-I function, resulting in enhanced viral replication (Li et al. 2020), vesicular stomatitis virus-induced miR-146a represses type I IFN production and promotes viral replication by suppressing TRAF6, IRAK2, and IRAK1 (Hou et al. 2009), and hepatitis C virus upregulates miR-208b and miR-499a-5p which enhances viral replication by dampening type I IFN signaling through suppression of the type I IFN receptor, IFNAR1 (Jarret et al. 2016). miRNA-mediated regulation of host immune responses is therefore complex, and while a growing number of functional studies have been conducted, our understanding of the broad functions host miRNAs play in antiviral responses remains limited.

Ranaviruses (family *Iridoviridae*) are large double-stranded DNA viruses causing emerging infectious diseases that threaten amphibian populations. Despite the devastating amphibian morbidities and mortalities associated with ranaviral infection, our understanding of frog antiviral defenses remains in its infancy, and the roles of frog miRNAs in regulating these antiviral responses are largely unexplored. As frog skin is an important barrier to pathogen entry (Varga et al. 2019), we have recently generated a *Xenopus laevis* (African clawed frog) dorsal skin epithelial-like cell line (Xela DS2) (Bui-Marinos et al. 2020) that is permissive to frog virus 3 (FV3), a member and type species of the *Ranavirus* genus, to facilitate our understanding of antiviral responses in frog skin epithelial cells (Bui-Marinos et al. 2021). FV3 enters cells by fusion at the plasma membrane (naked virions) or receptor-mediated endocytosis (enveloped virions) (Houts et al. 1974; Kelly 1975; Gendrault et al. 1981; Braunwald et al. 1985), the latter of which is believed to involve class A scavenger receptors (Vo et al. 2019). FV3 replicates its dsDNA genome in the nucleus and cytoplasm (Goorha et al. 1978) and produces viral double-stranded RNA (dsRNA) during its replicative cycle (Doherty et al. 2016). Thus, FV3 infection can be recognized by cytosolic pattern recognition receptors (PRRs) such as cGAS (dsDNA) or RIG-I/MDA5 (dsRNA). Along with others, we have studied frog cell antiviral responses through treatment with poly(I:C) (Sang et al. 2016; Wendel et al. 2018; Bui-Marinos et al. 2020), a synthetic viral dsRNA analog and known inducer of type I IFNs. Extracellular poly(I:C) is recognized by cell surface receptors and trafficked into the endosome for TLR3 recognition (Matsumoto and Seya 2008). While poly(I:C) is not a perfect mimic of viral dsRNA, as the length of viral dsRNA is known to impact the induction of host antiviral responses in aquatic vertebrates (Poynter and DeWitte-Orr 2015, 2018) and viral infection may stimulate a variety of different PRRs (e.g., cytosolic viral nucleic acid sensors), it permits comparisons of type I IFN responses across cell types and species. Modeling antiviral responses in frogs using poly(I:C) can further our understanding of how miRNAs function to regulate effective antiviral responses. By comparing poly(I:C)-stimulated antiviral miRNA responses in frog skin epithelial cells to antiviral miRNA responses to immunoevasive viruses such as FV3, we aim to elucidate how viral pathogens may subvert post-transcriptional regulatory responses as direct or indirect mechanisms of immunoevasion.

In this study, we sought to perform initial investigations into the role of host miRNAs in innate antiviral immune responses in frog skin epithelial cells. The goals of this study were to (*i*) profile changes in miRNA expression in a Xela DS2 skin epithelial-like cell line during antiviral responses to poly(I:C) and FV3; (*ii*) determine the antiviral targets of differentially expressed miRNAs; (*iii*) compare antiviral miRNA responses modeled by poly(I:C)—a known inducer of robust antiviral responses—to miRNA responses induced by FV3, an immunoevasive virus; and (*iv*) expand the number of currently annotated frog miRNAs through the discovery of novel *X. laevis* miRNAs.

Materials and methods

Cell line maintenance

Xela DS2, a skin epithelial-like cell line previously generated from *X. laevis* dorsal skin (Bui-Marinos et al. 2020), was maintained in seven parts Leibovitz's L-15 medium (Wisent, Mont-Saint-Hilaire, Canada) diluted with 3 parts sterile cell culture water to adjust for amphibian osmolarity, and is herein referred to as amphibian L-15 (AL-15) medium. AL-15 medium was supplemented with 15% fetal bovine serum (FBS; lot #234K18; VWR, Radnor, United States) and used to culture Xela DS2 cells at 26 °C in 75 cm^2 plug-seal tissue-culture treated flasks (BioLite, Thermo Fisher Scientific, Waltham, United States). Cells were split 1:4 upon reaching ~90%–95% confluency, which usually occurred every 3–4 d. Epithelioma Papulosum Cyprini (EPC) cells were maintained in Leibovitz's L-15 medium supplemented with 10% FBS. EPC cells were cultured in 75 cm^2 plug-seal tissue-culture treated flasks at 26 °C and were split 1:4 weekly. Prior to use in experiments, viable Xela DS2 and EPC cells were enumerated using Trypan blue (0.2% final concentration; Invitrogen, Waltham, United States) and a haemocytometer, and seeded to account for their respective plating efficiencies (79% for Xela DS2 and 100% for EPC).

Propagation of FV3 and determination of FV3 viral titres

FV3 (Granoff strain) was propagated in EPC cells as described previously (Bui-Marinos et al. 2021). Briefly, a monolayer of EPC cells was infected with a 1:10 dilution of stock FV3 in L-15 medium supplemented with 2% FBS for seven days at 26 °C. Seven days post-infection, virus-containing cell culture medium was collected, centrifuged at 1000 × *g* for 10 min, and filtered through a 0.22 µm PES filter (FroggaBio, Concord, Canada) prior to storage at −80 °C until use.

The tissue culture infectious dose values, wherein 50% of cells are infected ($TCID_{50}$/mL), were determined according to the modified Kärber method (Kärber 1931; Pham et al. 2011). EPC cells (100 000/well) were seeded in a 96-well plate (BioBasic, Toronto, Canada) and allowed to adhere overnight at 26 °C. The following day, cell culture medium was removed, and cells were treated with 200 µL of a 10-fold dilution series of the virus-containing cell culture supernatants to be tested (FV3 stock prepared as described above or experimental sample supernatant) diluted in L-15 medium containing 2% FBS. Plates were sealed with parafilm and incubated at 26 °C for seven days prior to visual examination of cytopathic effects (CPE). EPC monoloayers were scored for CPE and approximate FV3 plaque forming unit (PFU)/mL values were calculated by multiplying $TCID_{50}$/mL values by a factor of 0.7 (Knudson and Tinsley 1974). PFU/mL values were used to calculate multiplicity of infection (MOI) (Knudson and Tinsley 1974). The FV3 stock used in this study was determined to have a $TCID_{50}$/mL value of 1.64×10^9.

Exposure of Xela DS2 to poly(I:C) or FV3

Xela DS2 cells (passages 77, 80, and 83; $n = 3$) were seeded into two 6-well plates (700 000 cells/well) in AL-15 medium supplemented with 15% FBS and allowed to form a monolayer overnight at 26 °C. The following day, cell culture medium was removed, and cells were treated with 2 mL of medium

alone (AL-15 supplemented with 2% FBS, two wells per plate) or medium containing FV3 at an MOI of 2 (FV3 infected, one well per plate). The amount of virus required to obtain an MOI of 2 was calculated by first converting $TCID_{50}$/mL values to PFU/mL values (Knudson and Tinsley 1974). The raw $TCID_{50}$ values added to the Xela DS2 cells, without conversion to PFUs, was 2.0×10^6. After 2 h of incubation at 26 °C, the medium was removed, cells were washed three times with 2 mL amphibian phosphate buffered saline (8 g/L sodium chloride, 0.5 g/L potassium chloride, 2.68 g/L sodium phosphate dibasic heptahydrate, 0.24 g/L potassium phosphate monobasic), and 2 mL of fresh AL-15 medium supplemented with 2% FBS was added to all wells. At this point, 1 µg/mL of poly(I:C) composed of low and high molecular weight molecules (cat # P1530; Sigma-Aldrich, Burlington, United States) was added to one of the untreated wells. Untreated, poly(I:C)-treated, and FV3-infected cells were incubated at 26 °C for 24 h, while another set of untreated and FV3-infected cells were incubated at 26 °C for 72 h. Prior to collection of medium to determine $TCID_{50}$/mL values and cells for RNA extraction, cell images were captured using a Leica DMi1 phase-contrast microscope fitted with an MC170 colour camera and LASX 4.8 software.

RNA isolation

Adherent Xela DS2 cells and any detached cells in suspension were harvested for total RNA isolation using the Monarch Total RNA Minipreps kit (New England Biolabs, Ipswich, United States) according to the manufacturer's recommended protocol. Suspension cells present in the cell culture medium were collected by centrifugation at $500 \times g$ for 2 min and the resulting cell culture medium was aspirated. Lysis buffer (800 µL) was added to each well and incubated with adherent cells for 2 min at room temperature. Lysed cells were transferred from the 6-well plates to microcentrifuge tubes containing the corresponding pelleted suspension cells. Cells were resuspended by pipetting and incubated for 2 min to permit cell lysis. At this stage, an exogenous miRNA (cel-miR-39 Spike-In kit; Norgen Biotek Corp., Thorold, Canada) was spiked in (99 fmol) to serve as a positive control for miRNA detection. On-column DNase I treatment was performed for enzymatic removal of residual genomic DNA according to the manufacturer's instructions, and elution was performed in nuclease-free water (50 µL). Total RNA was quantified using the Take3 microvolume plate accessory on a Cytation 5 Cell Imaging Multi-Mode Reader (Biotek, Winooski, United States), RNA purity was determined by analyzing $A_{260/280}$ and $A_{260/230}$ ratios, and RNA integrity was examined by electrophoresis on a bleach agarose gel (Aranda et al. 2012).

Reverse transcription polymerase chain reaction (RT-PCR) detection of a control spike-in miRNA prior to small RNA-seq

For RT-PCR analysis of cel-miR-39 expression, 500 ng of DNase I-treated total RNA was reverse-transcribed into cDNA using the microScript miRNA cDNA Synthesis Kit (Norgen Biotek Corp., Thorold, Canada). Resulting cDNA was diluted four-fold and subjected to end-point PCR using Taq DNA Polymerase (GeneDirex Inc., Taoyuan, Taiwan) in a Mastercycler Nexus (Eppendorf, Hamburg, Germany) thermocycler. PCR reaction conditions were as follows: 1× GeneDirex buffer, 200 µM dNTPs, 0.2 µM forward and reverse primers, 0.625 U GeneDirex Taq, and 2 µL diluted cDNA. Spiked-in cel-miR-39 transcripts were amplified to confirm the ability to detect miRNAs, while *actb* transcripts were amplified as an internal control for amplifiability. PCR cycling conditions were as follows: 94 °C for 3 min, 40 × [94 °C for 15 s, 60 °C for 30 s, 72 °C for 45 s], and a final hold at 4 °C. All primers used in this study are listed in **Supplementary Table S1**.

Small RNA library preparation and sequencing

For each sample, ~2 µg of RNA (~80 ng/µL in 25 µL) was shipped to The Centre for Applied Genomics (TCAG) at The Hospital for Sick Children (Toronto, Canada) on dry ice. TCAG performed further quality assessment using a Bioanalyzer 2100 and RNA 6000 Nano LabChip Kit (Agilent

Technologies Inc., Santa Clara, United States), and samples with an RNA integrity number >8.5 were used for small RNA-seq library preparation. Library preparation and sequencing was performed by TCAG. Small RNA-seq libraries were prepared using the NEBNext Multiplex Small RNA Library Prep Set for Illumina (New England Biolabs, Ipswich, United States). Small RNAs were enriched using bead-based size selection. Resulting small RNA libraries were sequenced on an Illumina HiSeq 2500 rapid-run flow cell to generate 50 nucleotide (nt) single-end reads.

Small RNA-seq read preprocessing and mapping

Raw ~50 nt single-end sequencing reads were adaptor-trimmed and size-filtered using Cutadapt (Martin 2011) with the following parameters: single-end reads, 3′ adaptor of AGATCGGAAGAGCACACGTCTGAACTCCAGTCAC, minimum length of 17, maximum length of 30. Read quality reports were generated using FastQC (Andrews 2010) with default parameters. High quality (Q > 34; 0.04% error rate) clean reads were mapped to the *X. laevis* genome (J strain; GCF_001663975.1) using Bowtie2 (Langmead and Salzberg 2012) with the following parameters: single-end reads, write aligned and unaligned reads to separate files, allow one mismatch, output in sequence alignment map (SAM) format. Reads that mapped to the *X. laevis* genome were retained for further analyses. Cutadapt, FastQC, and Bowtie2 were run using the Galaxy web platform (usegalaxy.org; (Afgan et al. 2016)).

Detection of novel X. laevis *miRNAs*

Novel *X. laevis* miRNAs were detected using miRDeep2 v0.1.3 (Friedländer et al. 2012). Aligned reads were collapsed into unique sequences using the mapper.pl script and reads with counts <10 in a given library were discarded for this purpose. Transcripts with read counts <10 are generally considered to be noise and are often removed prior to downstream bioinformatics analysis (Law et al. 2016); thus, removing these reads prior to novel miRNA prediction helps improve the signal-to-noise ratio, which is an important component of miRDeep2-based miRNA detection. The miRDeep2.pl script was executed using default parameters and the following inputs: collapsed reads, alignments, the *X. laevis* genome, known *X. laevis* pre-miRNAs (miRBase), and known *X. laevis* and *Xenopus tropicalis* (Western clawed frog) miRNAs (miRBase). Secondary structures associated with novel *X. laevis* pre-miRNAs were determined using the RNAFold component of the ViennaRNA package v2.4.17 (Lorenz et al. 2011) under default parameters. Novel *X. laevis* miRNAs were considered high confidence if they were characterized by a miRDeep2 score ≥ 4 (≥ 90% probability of being a true positive) or if their sequence perfectly matched a known *X. tropicalis* miRNA.

Quantification and differential expression analysis of known and novel X. laevis *miRNAs*

X. laevis miRNA read counts were generated using miRDeep2 (Friedländer et al. 2012). Collapsed *X. laevis* reads, known and novel *X. laevis* miRNA sequences, and *X. laevis* pre-miRNA sequences (known (retrieved from miRBase) and novel (predicted by miRDeep2)) were input into the miRDeep2 quantifier.pl script using default parameters. Reads corresponding to several miRNAs were in very low relative abundance (e.g., <10 in a given library). To improve the accuracy of our analyses by strengthening the signal-to-noise ratio (Law et al. 2016), miRNAs were considered detected if their read counts were at least 10 in at least one library. miRNAs with <10 read counts in all libraries were considered undetected and were excluded from downstream analyses. Read counts served as input for differential expression analysis using DESeq2 (Love et al. 2014) and EdgeR (Robinson et al. 2010). DESeq2 parameters included "select datasets per level", input data = count data, and visualizing results = yes. EdgeR parameters included "single count matrix", use factor information file = yes, use gene annotation = no, normalization method = TMM. Known and novel *X. laevis* miRNAs were

considered differentially expressed if a false discovery rate (FDR) <0.05 was reached by both programs (consensus DE). Heatmaps were generated using heatmap2 with the following parameters: enable data clustering = no, coloring groups = blue to white to red. DESeq2, EdgeR, and heatmap2 were run using the Galaxy web platform (usegalaxy.org; (Afgan et al. 2016)).

miRNA target prediction

X. laevis 3′ UTRs were retrieved from the University of California Santa Cruz (UCSC) Table Browser using the Xenbase trackhub (genome.ucsc.edu; genome assembly v9.2). FV3 coding sequences (cds) were retrieved from National Center for Biotechnology Information (NCBI) (Accession NC_005946.1). Prior to running target prediction analysis, the dinucleotide frequencies of *X. laevis* 3′ UTRs and FV3 cds were calculated using the compseq function of EMBOSS v6.6.0 (Rice et al. 2000). Using these frequencies in target prediction analyses improves *p*-value accuracy (Rehmsmeier et al. 2004). The targets of known and novel *X. laevis* miRNAs were predicted using RNAcalibrate and RNAhybrid v2.1.2 (Rehmsmeier et al. 2004). RNAcalibrate was first used to estimate distribution parameters using default parameters (in addition to strict seed pairing at bases 2–7 of the miRNA and the dinucleotide frequencies generated by EMBOSS). Next, RNAhybrid was used to predict the *X. laevis* and FV3 mRNA targets of known and novel *X. laevis* miRNAs. RNAhybrid parameters included maximum energy = −25 kcal/mol, maximum mismatches in internal loop = 1, strict seed pairing at miRNA bases 2–7, mismatches in bulge loop = 0, one hit per interaction, $p < 0.01$. Gene functions were annotated using Xenbase (Karimi et al. 2018). Immune-related *X. laevis* targets were identified through a combination of manual search and cross-referencing The Gene Ontology (GO) Resource (The Gene Ontology Consortium 2019) and InnateDB (Breuer et al. 2013).

GO analysis

The PANTHER overrepresentation test was used to perform GO term enrichment analysis to reveal biological processes that are overrepresented in the list of *X. laevis* genes predicted to be targeted by differentially expressed *X. laevis* miRNAs (The Gene Ontology Consortium 2019). PANTHER parameters were as follows: reference list: all genes in database, "GO biological process complete" annotation dataset, Fisher's exact test, FDR <0.05. GO term analysis was performed at geneontology.org.

Reverse transcription quantitative polymerase chain reaction (RT-qPCR)

RT-qPCR experiments were performed on a duplicate set of RNA samples isolated from cells treated in parallel with RNA-seq samples. Total RNA (1 µg) was reverse-transcribed using the microScript miRNA cDNA synthesis kit (Norgen Biotech Corp., Thorold, Canada) according to the manufacturer's recommended protocol. Resulting cDNA was diluted (1/20) with nuclease-free water and stored at −20 °C until RT-qPCR analysis. RT-qPCR reactions consisted of 1 × PowerUP SYBR green mix (Thermo Fisher Scientific, Waltham, United States), 2.5 µL of diluted cDNA, and 500 nM (each) forward (miRNA-specific) and reverse (universal) primers in a final reaction volume of 10 µL. RT-qPCR primer sequences and efficiencies are presented in **Supplementary Table S1**. All RT-qPCR reactions were performed in triplicate on a QuantStudio5 Real-Time PCR System (Thermo Fisher Scientific, Waltham, United States), and reaction conditions were as follows: denaturation at 50 °C for 2 min and 95 °C for 2 min, followed by 40 cycles of denaturation at 95 °C for 1 s and extension at 60 °C for 30 s. A melt curve step (denaturation at 95 °C for 1 s and dissociation analysis at 60 °C for 20 s followed by 0.1 °C increments from 60 °C to 95 °C at 0.1 °C/s) was used to ensure the presence of a single dissociation peak.

RT-qPCR data were analyzed using the ΔΔCt method in Microsoft Excel with xla-miR-16a-5p serving as an endogenous control. xla-miR-16a-5p was chosen as a control for RT-qPCR normalization by

examination of the small RNA-seq data (normalized reads per million (RPM) read counts generated by the miRDeep2 quantifier.pl script). This control miRNA was chosen based on the following criteria: (*i*) <10% variability in expression (relative to total number of host-mapped reads) between experimental libraries and their respective control libraries and (*ii*) >1000 RPM in the libraries of at least one treatment. xla-miR-16a-5p served as the endogenous control for RT-qPCRs targeting miRNAs, as well as *dicer1* and *drosha* transcripts. While we recognize that normalization of an mRNA to a miRNA control is not ideal, it is difficult to identify an appropriate endogenous control gene for use in infection experiments, particularly late in viral infection. As the relative proportion of host RNA in total RNA samples decreases as viral RNA levels increase in infected cells, it is difficult to experimentally validate an endogenous control gene by RT-qPCR alone, due to the inherent instability of host RNA abundance between untreated and infected cells. Therefore, small RNA-seq data was used to determine an appropriate endogenous control miRNA in lieu of an mRNA control gene, which permitted accurate assessment of the stability of the control miRNA relative to the total host RNA abundance in each sample. Statistically significant differences were identified using one-way ANOVA tests paired with Dunnett's post-hoc tests or Student's *t*-tests where appropriate, and differences were considered statistically significant if $p < 0.05$.

Data availability

The small RNA-seq datasets generated by this study are available in the NCBI Short Read Archive repository (BioProject ID #PRJNA752644).

Results

Detection of *X. laevis* miRNAs in small RNA-seq libraries

To identify miRNAs that are involved in antiviral responses in frog skin epithelial cells, small RNAs from untreated (24 h and 72 h), poly(I:C)-treated (24 h), and FV3-infected (24 h and 72 h) Xela DS2 skin epithelial-like cells were sequenced. A poly(I:C) concentration of 1 µg/mL and a treatment duration of 24 h were chosen as these conditions produce robust transcriptional immune responses in Xela DS2 cells (Bui-Marinos et al. 2020), pretreatment with poly(I:C) confers functional protection against FV3 infection in Xela DS2 (Bui-Marinos et al. 2021), and similar concentrations have been used in previous studies profiling miRNA responses to poly(I:C) treatment in other species (Wang et al. 2017; Wu et al. 2019). Poly(I:C), comprised of a mixture of low molecular weight and high molecular weight molecules, was used to roughly mimic the viral RNAs of various lengths produced during FV3 replication (Tan et al. 2004). An FV3 MOI of 2 was chosen to approach a synchronous infection of Xela DS2 (approximately 86% of cells should receive one or more viral particles as calculated using the Poisson distribution), and thus facilitate the detection of host miRNAs in response to viral infection while minimizing potential cytotoxic effects of higher doses of the virus. In the present study, we opted not to examine FV3 infection of Xela DS2 cells at a lower MOI as that would result in an asynchronous infection and may obscure information that could be obtained regarding the timing of cellular miRNA expression in relation to progression of viral replication within host cells. Sampling time points of 24 h and 72 h were chosen to capture differences in antiviral responses at different times post infection as overt FV3-induced CPE are not obvious at earlier time points (e.g., 12 h), moderate CPE is observed at 24 h, and extensive CPE is evident at 72 h in Xela DS2 cells infected with FV3 at an MOI of 2 (**Supplementary Fig. S1a**). A later time point (i.e., 96 h) was not included based on previous observations of loss of cell viability in FV3-infected cells (Bui-Marinos et al. 2021). The $TCID_{50}$/mL values measured following FV3 infection of Xela DS2 cells at an MOI of 2 for 24 h or 72 h were 6.95×10^5 ($\log_{10} = 5.84$) or 2.81×10^7 ($\log_{10} = 7.44$), respectively (**Supplementary Fig. S1b**). Small RNAs were sequenced on an Illumina HiSeq 2500 resulting in 15 small RNA libraries ($n = 3$ per treatment; **Supplementary Fig. S1c–d**). A schematic of the bioinformatics pipeline

employed in this study is depicted in **Fig. 1a**. Approximately 7.6–11.3 million raw reads per sample underwent adapter, length, and quality filtering using Cutadapt (Martin 2011) and FastQC (Andrews 2010) to obtain ~1.5–5.9 million clean reads (17–30 nt) per library (**Fig. 1b**). Genome alignment was performed using Bowtie2 (Langmead and Salzberg 2012). Reads that aligned to the *X. laevis* genome were subjected to further analyses. The number of *X. laevis*-mapped reads in each library ranged from ~29% to 97% (**Fig. 1b**), and their size distribution spanned from 17 nt to 30 nt (**Fig. 1c**). More than 79% of the small RNA reads that mapped to the *X. laevis* genome were 21–24 nt in length, with 22–23 nt RNAs representing the majority.

At present, there are 247 mature *X. laevis* miRNAs in the miRBase database (Kozomara et al. 2019), a number which is relatively low for vertebrates. Thus, we sought to first identify novel *X. laevis* miRNAs from the small RNA libraries. Using miRDeep2 software, 133 novel *X. laevis* miRNAs were detected, which were classified into 52 families (**Supplementary Table S2**). Twenty-five of these novel *X. laevis* miRNAs are conserved in other species and present in miRBase, while the remainder are entirely novel miRNAs in any species (**Fig. 1d**). Many of these entirely novel miRNAs are derived from repetitive genomic regions (**Supplementary Table S2**). Conserved miRNAs were assigned the name of the corresponding orthologous miRNA in miRBase (Kozomara et al. 2019), while truly novel miRNAs were numbered sequentially and given the prefix "novel". There is a bias towards "U" as the first (5′) nucleotide of these novel *X. laevis* miRNAs, which is characteristic of vertebrate miRNAs (Yang et al. 2011). Next, miRDeep2 software was used to detect and quantify known and novel *X. laevis* miRNAs in each library. Along with the 133 novel *X. laevis* miRNAs, 136 known *X. laevis* miRNAs were detected across all 15 libraries (**Fig. 1d**). Thus, a total of 269 *X. laevis* miRNAs were detected in the small RNA-seq datasets. Most of these miRNAs were shared amongst all groups; however, two miRNAs were uniquely detected in FV3-infected cells at 24 h and 72 h, while one miRNA was uniquely detected in untreated cells at 72 h (**Fig. 1e**).

X. laevis miRNAs are differentially expressed in response to poly(I:C) and target important regulators of antiviral immunity

To begin elucidating the importance of frog miRNAs to innate antiviral responses, we profiled changes in *X. laevis* miRNA expression in response to the viral dsRNA analogue poly(I:C). Poly(I:C) was chosen to model antiviral responses in frog skin epithelial cells as poly(I:C) is a potent inducer of type I IFNs and downstream antiviral responses in Xela DS2 cells (Bui-Marinos et al. 2020) and in other vertebrate systems from humans to fish (Tamassia et al. 2008; Poynter and DeWitte-Orr 2015). Furthermore, prior treatment of Xela DS2 with low doses of extracellular poly(I:C) induces functional protective antiviral responses against FV3 (Bui-Marinos et al. 2021). Thus, poly(I:C) represents a suitable molecule to use in modeling potent and functional antiviral responses involving miRNAs for comparison with FV3-induced responses, which may be less representative of an effective miRNA-mediated antiviral response given that FV3 is immunoevasive (Grayfer et al. 2015; Robert et al. 2017).

Differential expression analysis was performed on the 269 (136 known and 133 novel) detected *X. laevis* miRNAs, comparing the 24 h untreated Xela DS2 libraries with poly(I:C)-treated Xela DS2 libraries. miRNAs were considered differentially expressed if differential expression was identified by both EdgeR and DESeq2 programs (consensus) and when FDR < 0.05. We discovered that 47 known *X. laevis* miRNAs are differentially expressed in response to poly(I:C) (23 downregulated and 24 upregulated) (**Fig. 2a**), while 18 novel *X. laevis* miRNAs are differentially expressed in response to poly(I:C) (seven downregulated and 11 upregulated) (**Fig. 2b**). These 65 miRNAs may represent key post-transcriptional mediators of effective innate antiviral responses in frog skin epithelial cells.

To begin identifying the potential functions of *X. laevis* miRNAs that are differentially expressed in response to poly(I:C), target prediction analyses were performed using RNAhybrid

(a)

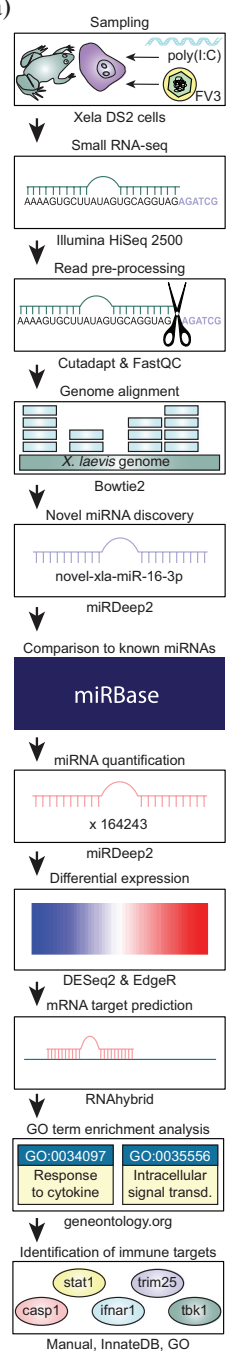

(b)

Library	Total reads	Filtered reads (17-30 nt)	Filtered reads aligned to *X. laevis* genome
Untreated 24 h #1	10,848,788	3,902,750	3,648,227 (93.48%)
Untreated 24 h #2	7,945,716	3,704,214	3,590,453 (96.93%)
Untreated 24 h #3	8,287,308	3,831,323	3,619,994 (94.48%)
Untreated 72 h #1	8,117,919	3,134,642	2,862,511 (91.32%)
Untreated 72 h #2	7,673,306	2,415,696	2,247,201 (93.02%)
Untreated 72 h #3	8,399,155	3,654,713	3,484,472 (95.34%)
poly(I:C)-treated 24 h #1	10,762,822	2,721,984	2,495,883 (91.69%)
poly(I:C)-treated 24 h #2	8,689,770	1,518,160	1,437,241 (94.67%)
poly(I:C)-treated 24 h #3	8,264,433	1,767,036	1,601,266 (90.62%)
FV3-infected 24 h #1	11,337,729	5,329,573	4,374,022 (82.07%)
FV3-infected 24 h #2	8,273,105	2,681,465	2,178,679 (81.25%)
FV3-infected 24 h #3	7,960,159	3,162,325	2,652,940 (83.89%)
FV3-infected 72 h #1	10,457,727	5,906,452	2,023,841 (34.26%)
FV3-infected 72 h #2	9,371,129	5,440,609	1,623,735 (29.84%)
FV3-infected 72 h #3	9,256,985	5,213,772	1,668,200 (32.00%)

(c)

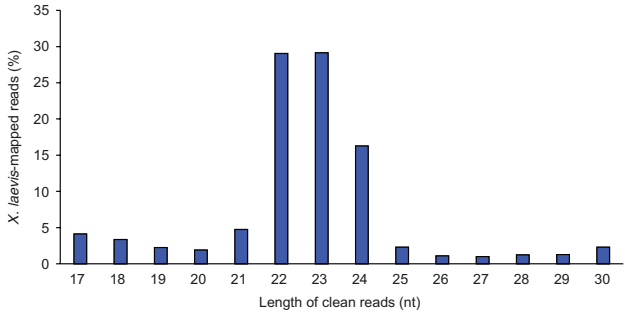

(d)

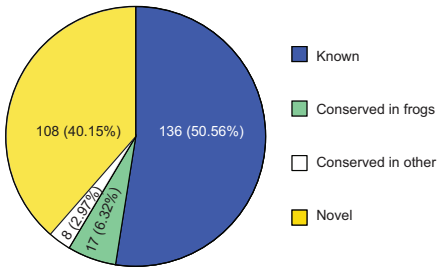

(e)

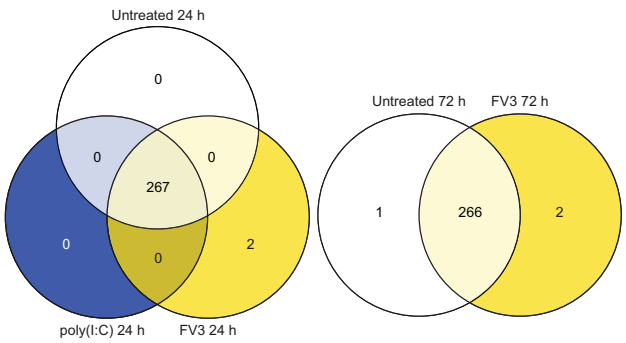

Fig. 1. Characteristics of *X. laevis* small RNA-seq libraries. (a) A schematic representation of the bioinformatics pipeline used in this study. (b) The total number of small RNA reads, the number of reads passing size filtering (17–30 nt), and the number of filtered reads that aligned to the *X. laevis* genome for all 15 small RNA libraries. Library numbers correspond to the respective independent experiment. (c) The size distribution of *X. laevis*-mapped reads across all libraries. (d) Different categories of miRNAs detected in Xela DS2 cells by small RNA-seq. "Known" miRNAs refer to *X. laevis* miRNAs present in miRBase, "conserved in frogs" refer to miRNA orthologs of known *X. tropicalis* miRNAs in miRBase not yet reported in *X. laevis*, "conserved in other" miRNAs refer to orthologs of miRNAs in miRBase not yet reported in frogs, and "novel" miRNAs refer to new miRNAs that are not present in miRBase in any species. (e) Venn diagram of the *X. laevis* miRNAs detected in small RNA-seq libraries generated from untreated, poly(I:C)-treated, and FV3-infected Xela DS2 cells (left = 24 h and right = 72 h).

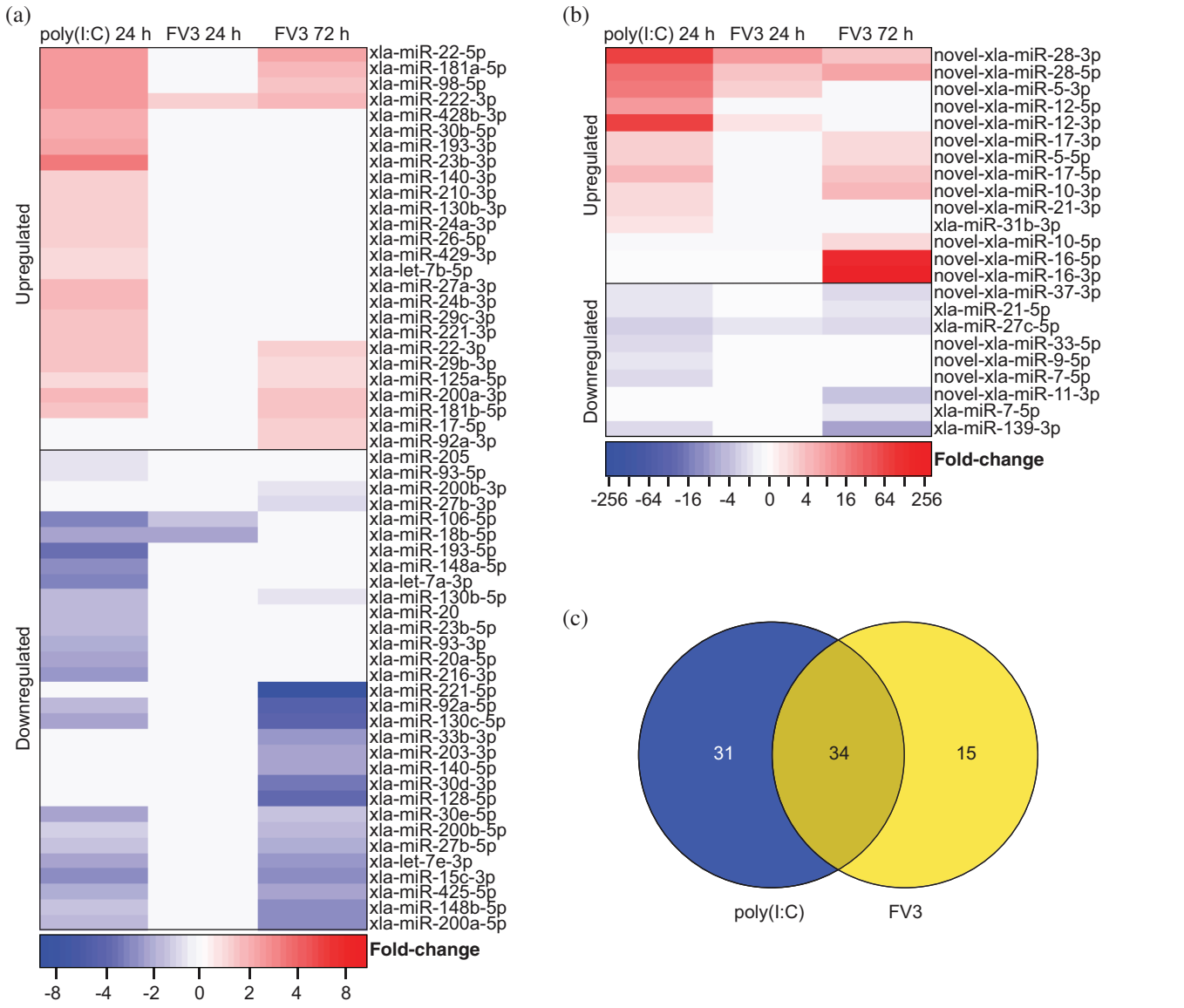

Fig. 2. Differential expression analysis of *X. laevis* miRNAs in response to poly(I:C) or FV3. Identification of (a) known and (b) novel *X. laevis* miRNAs that are differentially expressed in Xela DS2 cells in response to poly(I:C) or FV3 (compared to untreated cells). Statistically significant (FDR < 0.05, $n = 3$, Wald test) decreases and increases in miRNA levels relative to corresponding untreated controls are represented by blue and red, respectively. The indicated fold-change values (average of three independent experiments, $n = 3$) were determined by DESeq2 but were also statistically supported by EdgeR. White bars represent relative fold-changes that were not statistically significant. (c) Venn diagram representing *X. laevis* miRNAs that are differentially expressed in response to poly(I:C) treatment and (or) FV3 infection.

(Rehmsmeier et al. 2004) to predict their host gene targets. Robust interactions were predicted between the 65 *X. laevis* miRNAs that are differentially expressed in response to poly(I:C) and the 3′ UTRs of 2066 endogenous host genes (1937 if consolidating the L and S homeologs) (**Supplementary Table S4**). GO analysis of the predicted *X. laevis* targets of miRNAs that are differentially expressed in response to poly(I:C) revealed statistical enrichment of numerous functional categories, including many related to antiviral defenses such as "negative regulation of I-kappaB

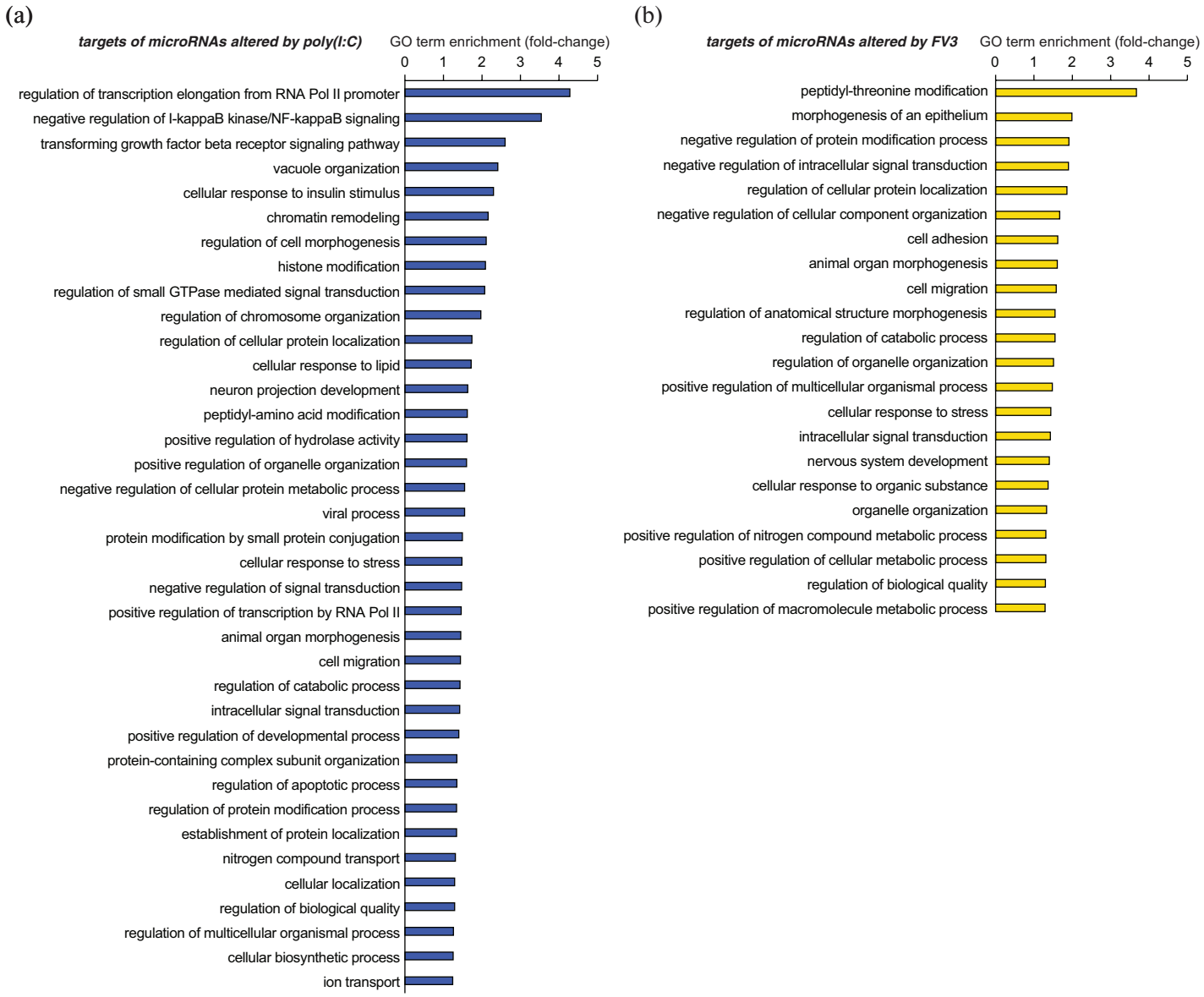

Fig. 3. GO term enrichment analysis of *X. laevis* 3′ UTRs predicted to be targets of differentially expressed *X. laevis* miRNAs. GO terms enriched in the list of targets of miRNAs with altered expression in response to (a) poly(I:C) or (b) FV3. In cases where multiple GO terms from the same hierarchy were found to be enriched, the most specific GO term is listed. An FDR value of less than 0.05 was considered statistically significant (Fisher's exact test).

kinase/NF-kappaB signaling", "transforming growth factor beta receptor signaling pathway", "viral process", "intracellular signal transduction", "cellular response to stress", and "regulation of apoptotic process" (Fig. 3a).

X. laevis miRNAs are differentially expressed in response to FV3 and target important regulators of antiviral immunity

We have recently demonstrated that Xela DS2 cells are permissive to FV3 but fail to induce antiviral programs in response to FV3 (Bui-Marinos et al. 2021). As FV3 is believed to be immunoevasive and

is known to produce dsRNA during its replication (Doherty et al. 2016), we sought to compare host miRNA responses to FV3 with host miRNA responses to poly(I:C) to develop an understanding of how FV3-induced miRNA responses differ from antiviral programs mounted in response to viral dsRNA. We profiled changes in *X. laevis* miRNA expression in response to FV3 infection and uncovered a total of 49 miRNAs that were differentially expressed in response to FV3 at either time point (24 h or 72 h). Three known miRNAs are differentially expressed in response to FV3 infection at 24 h (two downregulated and one upregulated), and 30 are differentially expressed in response to FV3 infection at 72 h (19 downregulated and 11 upregulated) (**Fig. 2a**). Five novel miRNAs are differentially expressed in response to FV3 infection at 24 h (one downregulated and four upregulated), and 15 are differentially expressed in response to FV3 infection at 72 h (six downregulated and nine upregulated) (**Fig. 2b**). While 34 of these differentially expressed miRNAs are also altered by poly(I:C) treatment, 15 are uniquely altered by FV3 infection (**Fig. 2c**). In addition, 31 miRNAs altered by poly(I:C) treatment were not altered by FV3 infection (**Fig. 2c**).

To elucidate the targets of miRNAs that are differentially expressed in response to FV3, target predictions were performed as described in the previous section, but also considered potential viral targets of these miRNAs. Robust interactions were predicted between five FV3 gene transcripts and five *X. laevis* miRNAs (three known and two novel) that are differentially expressed in response to FV3 (**Supplementary Table S3**), suggesting that *X. laevis* miRNAs that are differentially expressed in response to FV3 infection may directly target FV3 viral transcripts. Additionally, robust interactions were predicted between the 3′ UTRs of 1482 *X. laevis* genes (1406 if consolidating the L and S homeologs) and 49 miRNAs that are differentially expressed in response to FV3 (**Supplementary Table S4**). These findings suggest that 49 *X. laevis* miRNAs may play a role in regulating endogenous gene expression in response to FV3. GO term enrichment analysis on the list of targets of miRNAs that are altered in response to FV3 revealed enrichment of several GO terms, a few of which are immune-related, such as "cellular response to stress", "intracellular signal transduction", and "cellular response to organic substance" (**Fig. 3b**). Overall, the miRNAs altered by FV3 infection were associated with fewer immune-related functional categories than miRNAs altered by poly(I:C).

Mapping of differentially expressed miRNAs to antiviral pathways

Pathogens are sensed by a variety of PRRs that are either cytosolic (e.g., cGAS, RIG-I/MDA5) or membrane-associated (e.g., toll-like receptors (TLRs)) and recognize pathogen-associated molecular patterns (PAMPs) such as viral nucleic acids (Mogensen 2009; Motwani et al. 2019). PAMP sensing by PRRs can initiate antiviral signaling cascades that culminate in the production of IFNs and inflammatory cytokines that combat infection (Mogensen 2009). To gain a clearer picture of the antiviral pathways targeted by miRNAs that are differentially expressed in response to poly(I:C) or FV3, we mapped these miRNAs onto several key antiviral pathways such as cGAS-STING, RIG-I/MDA5, TLR3, TLR4, TLR7, TLR8, TLR9, and type I IFN signaling pathways (**Fig. 4**). Poly(I:C)-altered miRNAs target components of all eight of these pathways (*stim1, trim25, tbk1, tram1, ripk1, tab2, irak2, irf5, nmi, ifnar1, stat1, ubr4,* and *pkc-δ*), as well as their downstream products such as NF-κB-induced genes and ISGs (**Fig. 4a**). On the other hand, FV3-altered miRNAs targeted fewer components of these pathways (*trim14, stim1, trim25, tbk1, tram1, ripk1, tab2, stat1, ubr4,* and *pkc-δ*) and fewer NF-κB-induced genes and ISGs (**Fig. 4b**). While some targets in these pathways are found in common between miRNAs altered by poly(I:C) and FV3, there are several distinct differences. Poly(I:C)-altered miRNAs uniquely target *irak2, irf5, nmi,* and *ifnar1*, while FV3-altered miRNAs uniquely target *trim14*. Interestingly, while several poly(I:C)-altered miRNAs target components of TLR7/8/9 signaling, FV3 is associated with a lack of changes in the expression of miRNAs targeting these pathways.

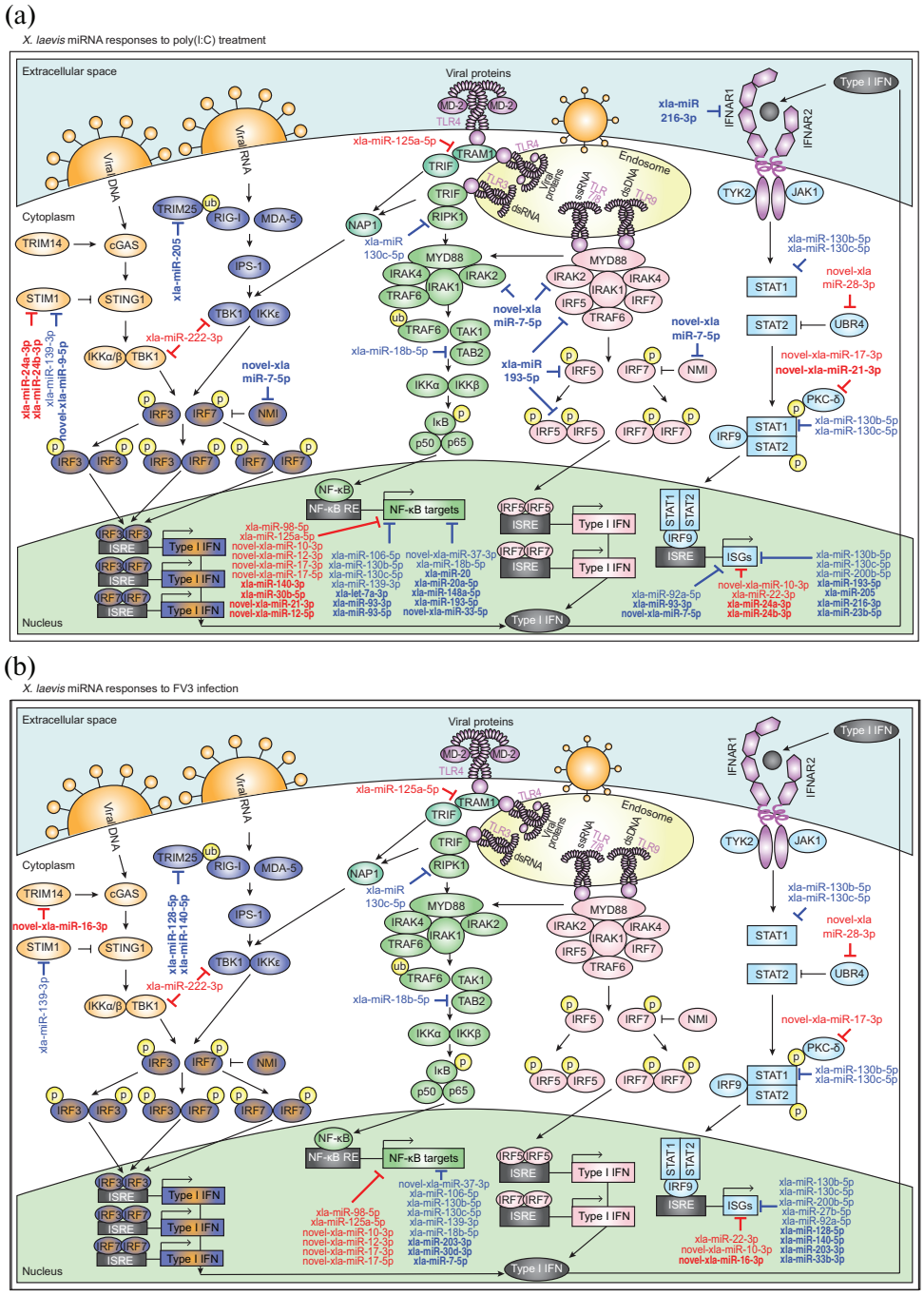

Fig. 4. Differentially expressed *X. laevis* miRNAs are predicted to target important regulators of innate antiviral immunity. Depicted are miRNAs that are predicted to target key genes in innate antiviral pathways and are differentially expressed in response to (a) poly(I:C) or (b) FV3. Upregulated miRNAs are in red and downregulated miRNAs are in blue. miRNAs with differential expression unique to either treatment are bolded. Pathway schematics were adapted from (InvivoGen). Note: IRF3 is produced and phosphorylated, and its activity stimulates type I IFN production (JAK-STAT pathway), which stimulates the production of IRF7 as an ISG (Marie et al. 1998; Sato et al. 1998). IRF7 is then phosphorylated and homodimerizes or heterodimerizes with phosphorylated IRF3 to enhance type I IFN production (Marie et al. 1998; Sato et al. 1998; Honda et al. 2006). dsDNA = double-stranded DNA; dsRNA = double-stranded RNA; IFN = interferon; ISGs = IFN-stimulated genes; ISRE = IFN-stimulated response element; NF-κB RE = NF-κB response element; p = phosphorylation; ssRNA = single-stranded RNA; ub = ubiquitination.

Validation of key differentially expressed miRNAs that target immune-related genes

RT-qPCR was used to validate the differential expression profiles of a subset of *X. laevis* miRNAs that are predicted to target important regulators of innate antiviral responses. Twelve miRNAs were chosen that (*i*) are predicted to target important immune-related genes; (*ii*) represent a combination of known, conserved, and novel miRNAs; (*iii*) represent a combination of upregulated and downregulated miRNAs; and (*iv*) represent a combination of miRNAs with changes in expression that are consistent between the poly(I:C) and FV3 treatment groups or are inconsistent between these groups. These miRNAs included xla-miR-106-5p, xla-miR-130c-5p, xla-miR-139-3p, xla-miR-140-5p, xla-miR-222-3p, novel-xla-miR-7-5p, xla-miR-22-5p, novel-xla-miR-12-3p, novel-xla-miR-16-5p, novel-xla-miR-16-3p, novel-xla-miR-28-5p, and novel-xla-miR-28-3p. The RNA-seq-derived differential expression profiles of 11 of these miRNAs were successfully validated by RT-qPCR (**Fig. 5**), and one miRNA (xla-miR-222-3p) did not show comparable differential expression profiles between the two techniques. With regards to the 11 validated profiles, there are a few cases where one technique produced results that were statistically significant whereas the other technique did not (xla-miR-106-5p in FV3-infected cells at 24 h and 72 h; novel-xla-miR-12-3p in FV3-infected cells at 72 h, novel-xla-miR-16-5p in FV3-infected cells at 24 h, and novel-xla-miR-16-3p in FV3-infected cells at 24 h). These are likely due to slight variation in replicates and differences in sensitivity of the two techniques. For example, novel-xla-miR-16-5p and novel-xla-miR-16-3p were undetected in untreated samples by RNA-seq, whereas amplification was achieved using RT-qPCR. The lack of detection in RNA-seq can slightly skew the fold-change values calculated. Despite the sometimes slight variance in magnitude of differential expression between the two techniques (RT-qPCR and RNA-seq), the overall trends remained the same.

Poly(I:C) treatment downregulates *dicer1* transcripts, while FV3 infection suppresses *dicer1* and *drosha* transcripts

miRNAs that target immune-related genes were more frequently downregulated than upregulated in response to either poly(I:C) or FV3. In line with this, and as observed in other pathosystems, host cells have been found to modulate global miRNA biogenesis to manipulate miRNA expression during infection (Bruscella et al. 2017). Thus, we sought to profile changes in the transcript levels of components of the miRNA biogenesis pathway, *dicer1* and *drosha*, in response to poly(I:C) or FV3. RT-qPCR analysis revealed downregulation of *dicer1* transcripts in response to poly(I:C) (24 h) as well as FV3 (24 and 72 h) (**Fig. 6a**). In addition, *drosha* transcripts were downregulated in response to FV3 infection at 72 h (**Fig. 6b**). Together, these results suggest that miRNA biogenesis is partially suppressed in response to viral infection.

Discussion

Modeling of conserved and robust antiviral responses involving miRNAs

We uncovered 80 *X. laevis* miRNAs that are differentially expressed in response to extracellular poly(I:C) and (or) FV3 in a frog skin epithelial-like cell line, suggesting for the first time that frog miRNAs are key regulators of antiviral immunity. Changes in miRNA expression in response to poly(I:C) were profiled to model robust antiviral responses, as poly(I:C) induces potent antiviral responses and is an inert molecule (nonimmunoevasive). Extracellular delivery of poly(I:C) is intended to mimic the viral dsRNA replicative products released into the extracellular space following lysis of infected cells and is subsequently sensed by neighboring cells. Poly(I:C) treatment of Xela DS2 cells altered the levels of 65 *X. laevis* miRNAs, which may play a role in post-transcriptional regulation

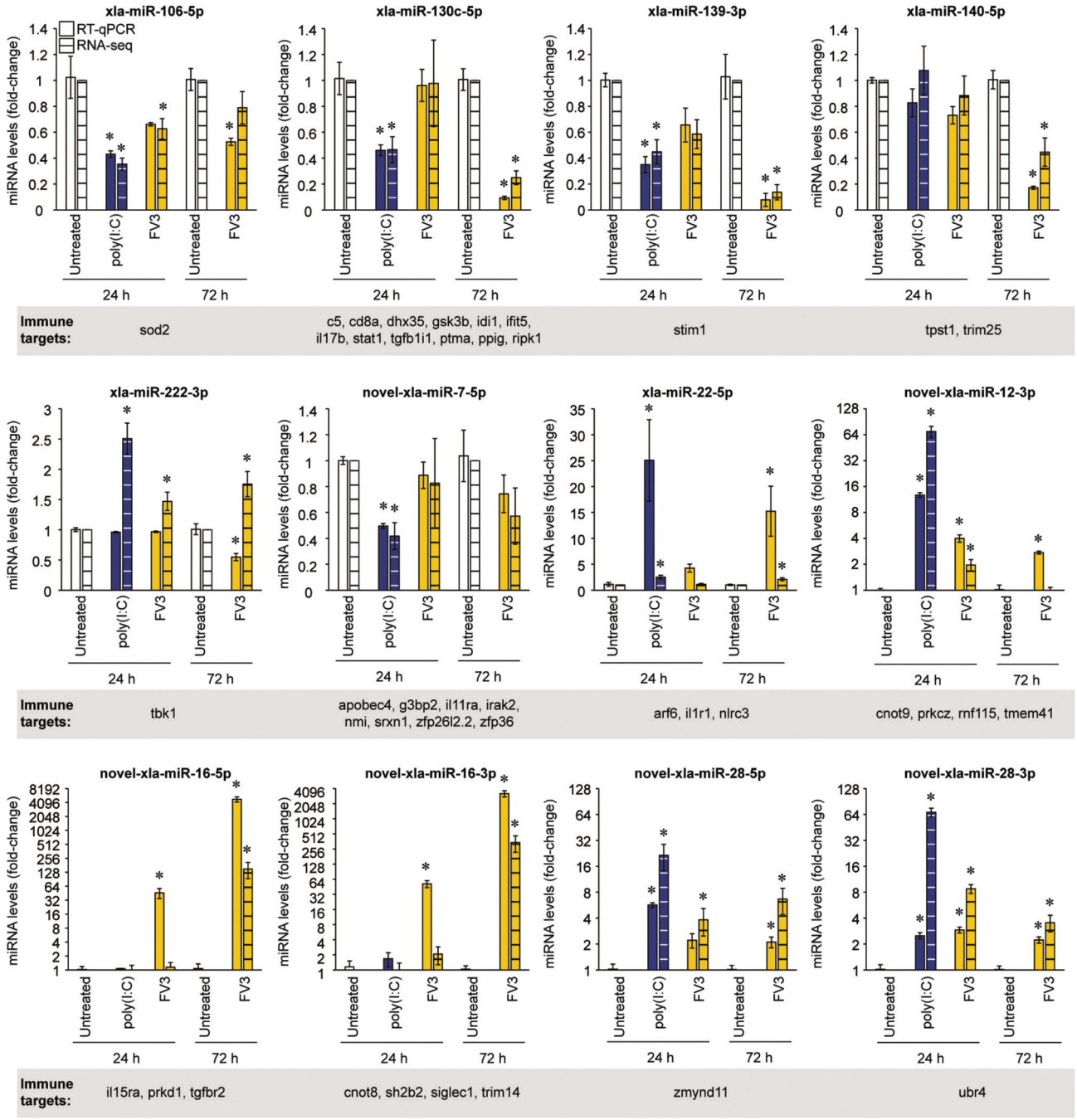

Fig. 5. RT-qPCR validation of a subset differentially expressed *X. laevis* miRNAs. cDNA synthesized from total RNA isolated from untreated, poly(I:C)-treated and FV3-infected Xela DS2 cells was subjected to RT-qPCR analysis using forward primers specific to each miRNA of interest and a universal reverse primer. RT-qPCR results are depicted in solid colours and differential expression analysis of the RNA-seq data is depicted in striped corresponding colours for comparison. RT-qPCR data were analyzed using the ΔΔCt method using xla-miR-16a-5p (levels unchanged by any treatment based on RNA-seq data) as an internal control. Data are depicted as mean ± standard error ($n = 3$), and values corresponding to treatment groups are presented relative to their respective untreated control, which was set to a reference value of 1. Statistical significance was assessed using one-way analysis of variance (ANOVA) tests paired with Dunnett's post-hoc tests (24 h) or unpaired Student's *t*-tests (72 h), with a p value < 0.05 considered statistically significant from the time-matched untreated control (within the same miRNA detection method), as denoted by asterisks (*). Immune gene targets of each miRNA predicted using RNAhybrid are depicted below the corresponding graph.

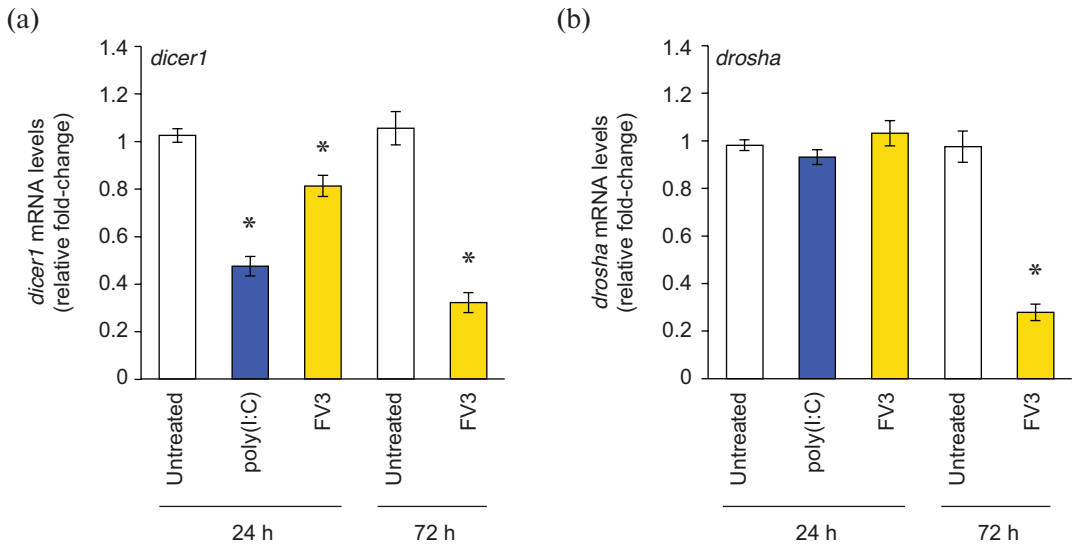

Fig. 6. Fold-change in *dicer1* and *drosha* mRNA transcript levels in response to poly(I:C) treatment or FV3 infection of Xela DS2 cells. cDNA generated from total RNA isolated from untreated, poly(I:C)-treated, or FV3-infected Xela DS2 cells was subjected to RT-qPCR analysis targeting (a) *dicer1* and (b) *drosha* transcripts. RT-qPCR data were analyzed using the ΔΔCt method using xla-miR-16a-5p (levels unchanged by any treatment based on RNA-seq data) as an internal control. Data are depicted as mean ± standard error ($n = 3$), and values corresponding to treatment groups are presented relative to their respective untreated control, which was set to a value of 1. Statistical significance was assessed using a one-way ANOVA paired with Dunnett's post-hoc test (24 h) or an unpaired Student's *t*-tests (72 h). A p value < 0.05 was considered statistically significant and asterisks (*) denote statistical difference from the time-matched untreated control.

of host gene expression in response to exogenous viral dsRNA. Poly(I:C) treatment of Xela DS2 induced changes in miRNAs that are predicted to target important regulators of antiviral signaling pathways such as cGAS-STING (e.g., *stim1*), RIG-I/MDA5 (e.g., *trim25*), TLR signaling (e.g., *irak2*, *irf5*, *ripk1*, and *tab2*), type I IFN signaling (e.g., *ifnar1* and *stat1*), NF-κB-induced genes (e.g., *tp53* and *sod2*), and ISGs (e.g., *adar* and *isg20l2*). It is important to note that the currently available *X. laevis* genome annotations remain incomplete, and immune genes are particularly under-annotated. Thus, while target predictions were performed with the most up-to-date annotation, our target prediction analysis may represent an underestimation of immune gene targets. Additionally, our analyses were restricted to 3′ UTRs, as although miRNAs have recently been shown to interact with 5′ UTRs and cds, the 3′ UTR is the location most often targeted by miRNAs (Lee et al. 2009; Fang and Rajewsky 2011). Nevertheless, targeting of these antiviral pathways is reflective of what has been observed in other vertebrates, where miRNAs that are differently expressed during immune responses have been found to target orthologs of these same immune genes (Boosani and Agrawal 2016). For example, miR-146a is induced by vesicular stomatitis virus in murine peritoneal macrophages (Hou et al. 2009) and targets *irak2* in mice (Hou et al. 2009) and *irf5* and *stat1* in humans (Tang et al. 2009); miR-155 is induced during inflammatory responses in humans and mice (O'Connell et al. 2007; Tili et al. 2007) and targets *ripk1* (Tili et al. 2007) and *tab2* (Imaizumi et al. 2010); miR-208b and miR-499a-5p are induced in human hepatocytes in response to hepatitis C virus infection and target *ifnar1* (Jarret et al. 2016); and miR-30a is induced in HeLa cells in response to coxsackievirus B3 and targets *trim25* (Li et al. 2020). Identification of these differentially regulated miRNAs set the foundation for future studies to systematically validate the existence of physical functional interactions between differentially expressed *X. laevis* miRNAs and their putative antiviral target genes.

Our data sheds light on conserved post-transcriptional responses to viral dsRNA and the potential for involvement of miRNAs that target a core set of conserved antiviral genes. For example, it has been shown in mammals that poly(I:C) induces Sod2 expression to combat reactive oxygen species (ROS), which are associated with viral infection (Molteni et al. 2014). However, the mechanism through which poly(I:C) induces Sod2 remains unknown. We identified a miRNA (xla-miR-106-5p) that targets *sod2* and is downregulated in response to poly(I:C). Similarly, human hsa-miR-106a-5p is also predicted to target Sod2. Thus, repression of xla-miR-106-5p may be a conserved mechanism through which Sod2 is induced to combat ROS accumulation in response to viral infection. In line with this, oxidative stress has been shown to repress miR-106-5p in humans (Tai et al. 2020), and downregulation of miR-106-5p has separately been shown to restore Sod activity to inhibit apoptosis and oxidative stress in rats (Li et al. 2017). Another interesting candidate is xla-miR-22-5p, which is upregulated by poly(I:C) treatment or FV3 infection and is predicted to target *arf6* (ADP-ribosylation factor 6), a gene known to regulate TLR9-mediated immune signaling in response to exogenous DNA (Wu and Kuo 2012). As Arf6 enhances proinflammatory cytokine production (Wu and Kuo 2012), upregulation of xla-miR-22-5p and subsequent suppression of *arf6* in response to viral infection may represent a strategy to modulate inflammation to prevent excessive cellular damage. Interestingly, *arf6* is a conserved target of the miR-22-5p orthologs in humans, mice, rats, cows, and the Western clawed frog. Together, these observations suggest that miRNA-mediated mechanisms of regulating innate immunity are highly conserved, even in distantly related vertebrates.

Immunoevasive viruses produce host miRNA profiles distinct from those associated with robust and effective antiviral responses

FV3 is immunoevasive (Grayfer et al. 2015; Robert et al. 2017) and does not elicit robust antiviral responses in Xela DS2 skin epithelial-like cells (Bui-Marinos et al. 2021). Thus, we sought to profile changes in miRNA expression in response to FV3 for comparison to poly(I:C)-induced miRNA alterations to identify potential miRNA-based mechanisms of immunoevasion. Accordingly, FV3-infection is associated with changes in the expression of fewer miRNAs compared to poly(I:C), such that only 34 of the 65 miRNAs altered by poly(I:C) treatment were also affected by FV3 infection. Thus, the 31 miRNAs that are altered by poly(I:C) treatment and not FV3 infection, along with the 15 miRNAs that are altered by FV3 infection and not poly(I:C) treatment, may play a role in FV3's ability to evade host immune systems in skin epithelial cells. In addition, some miRNA changes evident at 24 h post-poly(I:C) treatment were not evident until 72 h post-FV3 infection, and fewer of the differentially expressed miRNAs in FV3-infected Xela DS2 cells are predicted to target immune genes compared to those altered by poly(I:C). These findings suggest that FV3 infection may be associated with a dampened and (or) delayed immune response, which is in accordance with the theory that FV3 possesses immunoevasion capabilities.

Comparing the antiviral targets of poly(I:C)-altered miRNAs and FV3-altered miRNAs reveals several notable differences. For example, poly(I:C) treatment suppresses the expression of several miRNAs that are predicted to target multiple components of TLR7, TLR8, and TLR9 pathways, a layer of regulation that appears to be absent in FV3-infected cells. As FV3 is a dsDNA virus and dsDNA is a TLR9 ligand, the possibility exists that FV3 may actively interfere with miRNA-mediated regulation of TLR9 signaling as a facet of immunoevasion. It is also interesting to note that compared to FV3 infection, poly(I:C) treatment affects the expression of more miRNAs that target NF-kB-regulated genes and ISGs. This suggests that FV3 may actively interfere with the regulation of antiviral genes that are typically induced in response to the activation of antiviral signaling pathways. Despite these intriguing observations, it is important to recognize the caveat that extracellular delivery of poly(I:C) can initiate antiviral pathways that may be distinct from the pathways stimulated by FV3 infection (e.g., poly(I:C) can activate endosomal TLR3 pathways while viral dsRNA produced during FV3 replicative cycles may activate cytosolic

sensing pathways such as RIG-I/MDA5). Additionally, numerous other viral components that are not mimicked by poly(I:C) (e.g., viral proteins, viral dsDNA) can be recognized by different PRRs. Thus, while extracellular poly(I:C) is not a perfect comparator, our previous studies have established that extracellular introduction of poly(I:C) activates antiviral pathways that lead to an effective antiviral response which protects against FV3 in Xela DS2 cells (Bui-Marinos et al. 2021) and serves to provide a reference for which miRNAs are regulated during an effective antiranaviral immune response. Future studies should examine miRNA profiles in response to poly(I:C) that is transfected into the cell, which may more closely approximate cytosolic PRR sensing of viral dsRNA replicative products.

To our knowledge, only one other study has simultaneously profiled changes in miRNA expression in response to poly(I:C) and an immunoevasive virus (porcine reproductive and respiratory syndrome virus (PRRSV)) (Wu et al. 2019). Similar to our observations, PRRSV infection of porcine alveolar macrophages resulted in alterations to only 33 of the 197 miRNAs found to be altered by poly(I:C) treatment (Wu et al. 2019). However, in contrast to the findings of the aforementioned study which did not detect any miRNAs altered by PRRSV infection that were not altered by poly(I:C) treatment, we detected differential expression of a handful of miRNAs in response to FV3 infection that were unaffected by poly(I:C) treatment. Of particular interest are two novel *X. laevis* miRNAs with no known orthologs in other species (novel-xla-miR-16-5p and novel-xla-miR-16-3p) that are strongly induced (150-fold and 342-fold, respectively, as measured by RT-qPCR) in response to FV3 but not poly(I:C). These novel miRNAs originate from the same pre-miRNA and are both predicted to target important genes involved in innate antiviral immunity, including *tgfbr2* (transforming growth factor beta receptor 2; novel-xla-miR-16-5p) and *trim14* (tripartite-containing motif 14; novel-xla-miR-16-3p). Tgfbr2 is a receptor for the well-studied TGF-β anti-inflammatory cytokine and viral induction of novel-xla-miR-16-5p may result in dampening of TGF-β signaling, preventing the host from limiting inflammatory responses to protect against cellular damage caused by excessive inflammation. Trim14 indirectly promotes type I IFN production by stabilizing the cytosolic dsDNA sensor cGAS (Chen et al. 2016). In the absence of Trim14, type I IFN antiviral responses are impaired (Chen et al. 2016). It is interesting to note that novel-xla-miR-16-3p was undetectable by RNA-seq in Xela DS2 cells that were not infected with FV3, but it is strongly induced in response to FV3 infection. As novel-xla-miR-16-3p targets a stabilizer of cGAS, which is a sensor of viral dsDNA, FV3 may force novel-xla-miR-16-3p expression to actively suppress cGAS signaling and evade recognition by the host immune system. Indeed, viral inhibition of cGAS signaling has been observed in other pathosystems (Eaglesham et al. 2019). Whether cGAS signaling is involved in responding to FV3 infection and the roles FV3-induced host miRNAs play in blocking cGAS signaling require further investigation.

Our study is the first to profile changes in host miRNA expression in response to ranavirus infection in skin cells modeled by a skin epithelial-like cell line, as the only other study that has profiled changes in host miRNAs in response to ranavirus infection was performed in spleen. Meng et al. (2018) profiled *Andrias davidianus* (Chinese giant salamander) miRNA responses to Chinese giant salamander iridovirus infection of spleen tissue and discovered numerous differentially expressed miRNAs predicted to target genes involved in important antiviral signaling pathways such as TLR, RIG-I/MDA5, and JAK-STAT pathways (Meng et al. 2018). Despite the similarities to pathways targeted in our study, only two miRNA families found to be differentially expressed in the study by Meng et al. (2018) were also found to be differentially expressed in response to FV3 in our study (miR-200 and miR-203, both downregulated). Thus, while the antiviral pathways targeted by miRNAs in response to different ranaviruses may mirror one another, it appears as though regulation of these pathways may be achieved using different miRNAs. Nevertheless, it will be important for future studies to verify that the differentially expressed miRNAs identified in our study function in antiviral responses and impact viral replication. As our study utilized a skin epithelial-like cell line, a potential limitation is that the findings may not be entirely representative of the complex processes

occurring in whole skin tissue. Thus, to broaden our understanding of miRNA-mediated antiviral responses in frog skin, future studies are required to identify the contribution of frog miRNAs to antiviral responses in other cell types present in frog skin, as well as in whole skin tissue.

In addition to targeting host antiviral genes, several differentially expressed miRNAs are predicted to target viral transcripts corresponding to a myristoylated membrane protein (FV3 ORF 53 R), LCDV1 orf2-like protein, and hypothetical proteins. FV3 ORF 53R has been suggested to interact with the host cellular membrane and is required for virion assembly (Whitley et al. 2010), and thus may represent an ideal molecule for the host immune system to target. It is important to note that our target prediction analyses were performed with FV3 cds, as the current FV3 genome annotation lacks defined 3′ UTRs. While viral cds are frequently targeted by host miRNAs (Wang et al. 2012; Zheng et al. 2013; Ho et al. 2016), our FV3 target predictions may represent a fraction of the total FV3 mRNAs targeted by host miRNAs.

Suppression of miRNA biogenesis as a facet of both effective immune responses and immunoevasion

Recent studies have shown that transient inhibition of miRNA biogenesis is critical during the activation of IFN responses in HeLa cells, and leads to reduced levels of specific miRNAs, many of which target innate immune genes (Witteveldt et al. 2018). Accordingly, our study revealed that the majority of differentially expressed miRNAs that target immune genes are downregulated rather than upregulated, and both poly(I:C) treatment and FV3 infection suppressed *dicer1* transcript levels. In line with this, studies have detected suppression of *dicer1* but not *drosha* in response to viral infection of human, nonhuman primate, and murine cells (vaccinia virus infection of HeLa, Vero, and 3T3 cells) (Grinberg et al. 2012). Therefore, transient Dicer suppression may constitute a conserved antiviral response. Interestingly, we observed downregulation of *drosha* transcript levels in response to FV3 but not poly(I:C), which raises the possibility that Drosha suppression may be linked to immunoevasion tactics employed by FV3. Accordingly, studies have demonstrated that during infection of human 293T cells with Sindbis virus or vesicular stomatitis virus, Drosha is shuttled to the cytoplasm and repurposed to cleave viral RNA to inhibit viral replication (Shapiro et al. 2014). Thus, it stands to reason that immunoevasive viruses may be equipped to restrict Drosha function to facilitate viral replication. A survey of the literature revealed that direct manipulation of Drosha expression by a virus has, to the best of our knowledge, not yet been reported. Thus, it is unclear whether Drosha is a common target of viral immunoevasion or whether it may be a target that is unique to FV3.

Expansion of the frog miRNAome

Our sequencing efforts expanded the number of currently annotated *X. laevis* miRNAs from 247 to 380. Of the 133 novel *X. laevis* miRNAs we identified in Xela DS2 cells, 108 have never been detected in any species before. While several novel miRNAs were differentially expressed in response to poly(I:C) or FV3, the majority were not. A large portion of the novel miRNAs that were not altered by poly(I:C) or FV3 originate from repetitive regions found across multiple chromosomes and may thus function in controlling repetitive elements. Indeed, miRNAs have been recently characterized as emerging regulators of transposable elements (Pedersen and Zisoulis 2016). Thus, our findings are likely to stimulate exciting studies in research areas outside of innate immunity.

While our study significantly increased the number of annotated *X. laevis* miRNAs, it is important to note that our novel miRNA discovery efforts have likely not completed the map of the *Xenopus* miRNAome, as miRNAs are often exclusively expressed in specific cell types, tissue types, developmental stages, or cellular contexts (e.g., infection) (Bartel 2004). Additionally, our novel miRNA discovery pipeline involved removing reads with <10 counts in a given library, which may exclude the

discovery of novel miRNAs expressed at low levels. However, removing reads with counts <10 improves the signal-to-noise ratio (Law et al. 2016) which enables the discovery of high confidence miRNAs (Friedländer et al. 2012), and this benefit arguably outweighs the limitation of missing some novel miRNAs.

Concluding remarks

To our knowledge, this study is the first to highlight the role of miRNAs in antiviral defenses within frog skin epithelial cells and sheds light on evolutionarily conserved post-transcriptional mechanisms of regulating antiviral responses in vertebrates. We identified poly(I:C)-induced antiviral responses involving miRNAs in frogs and uncovered differences between these responses and miRNA-mediated responses to the immunoevasive FV3. Our findings further our understanding of frog-FV3 interactions by identifying miRNAs as an added layer of antiviral gene regulation in frogs and uncovering the possibility that ranaviruses may hijack specific host miRNAs to facilitate immunoevasion. Future functional studies will be instrumental in solidifying these initial observations, and similar studies in other cell types and tissues will be crucial to uncovering cell type- and tissue-specific antiviral miRNA responses in frogs.

Funding

This study was supported by a Natural Sciences and Engineering Research Council of Canada (NSERC) Discovery Grant (RGPIN-2017-04218) and University of Waterloo Start-Up Funds to B.A.K. and an NSERC Postdoctoral Fellowship (PDF-546075-2020) to L.A.T.

Author contributions

LAT and BAK conceived and designed the study. LAT and MPB-M performed the experiments/collected the data. LAT and BAK analyzed and interpreted the data. BAK contributed resources. LAT, MPB-M, and BAK drafted or revised the manuscript.

Competing interests

The authors declare they have no conflicts of interest.

Data availability statement

All relevant data are within the paper and in the Supplementary Material.

Supplementary material

The following Supplementary Material is available with the article through the journal website at doi:10.1139/facets-2021-0090.

Supplementary Material 1

References

Afgan E, Baker D, van den Beek M, Blankenberg D, Bouvier D, Čech M, et al. 2016. The Galaxy platform for accessible, reproducible and collaborative biomedical analyses: 2016 update. Nucleic Acids Research, 44(W1): W3–W10. DOI: 10.1093/nar/gkw343

Andrews S. 2010. FastQC: A quality control tool for high throughput sequence data [online]: Available from bioinformatics.babraham.ac.uk/projects/fastqc/.

Aranda PS, LaJoie DM, and Jorcyk CL. 2012. Bleach gel: a simple agarose gel for analyzing RNA quality. Electrophoresis, 33(2): 366–369. DOI: 10.1002/elps.201100335

Bartel DP. 2004. MicroRNAs: genomics, biogenesis, mechanism, and function. Cell, 116(2): 281–297. DOI: 10.1016/s0092-8674(04)00045-5

Boosani CS, and Agrawal DK. 2016. Epigenetic Regulation of Innate Immunity by microRNAs. Antibodies (Basel), 5(2). DOI: 10.3390/antib5020008

Braunwald J, Nonnenmacher H, and Tripier-Darcy F. 1985. Ultrastructural and biochemical study of frog virus 3 uptake by BHK-21 cells. Journal of General Virology, 66(Pt 2): 283–293. DOI: 10.1099/0022-1317-66-2-283

Breuer K, Foroushani AK, Laird MR, Chen C, Sribnaia A, Lo R, et al. 2013. InnateDB: systems biology of innate immunity and beyond–Recent updates and continuing curation. Nucleic Acids Research, 41(Database issue): D1228–D1233. PMID: 23180781 DOI: 10.1093/nar/gks1147

Bruscella P, Bottini S, Baudesson C, Pawlotsky JM, Feray C, and Trabucchi M. 2017. Viruses and miRNAs: More Friends than Foes. Frontiers in Microbiology, 8: 824. PMID: 28555130 DOI: 10.3389/fmicb.2017.00824

Bui-Marinos MP, Todd LA, Wasson MD, Morningstar BEE, and Katzenback BA. 2021. Prior induction of cellular antiviral pathways limits frog virus 3 replication in two permissive *Xenopus laevis* skin epithelial-like cell lines. Developmental and Comparative Immunology, 124: 104200. PMID: 34237380 DOI: 10.1016/j.dci.2021.104200

Bui-Marinos MP, Varga JFA, Vo NTK, Bols NC, and Katzenback BA. 2020. Xela DS2 and Xela VS2: Two novel skin epithelial-like cell lines from adult African clawed frog (*Xenopus laevis*) and their response to an extracellular viral dsRNA analogue. Developmental and Comparative Immunology, 112: 103759. PMID: 32526291 DOI: 10.1016/j.dci.2020.103759

Chen M, Meng Q, Qin Y, Liang P, Tan P, He L, et al. 2016. TRIM14 inhibits cGAS degradation mediated by selective autophagy receptor p62 to promote innate immune responses. Molecular Cell, 64(1): 105–119. DOI: 10.1016/j.molcel.2016.08.025

Doherty L, Poynter SJ, Aloufi A, and DeWitte-Orr SJ. 2016. Fish viruses make dsRNA in fish cells: characterization of dsRNA production in rainbow trout (*Oncorhynchus mykiss*) cells infected with viral haemorrhagic septicaemia virus, chum salmon reovirus and frog virus 3. Journal of Fish Diseases, 39(9): 1133–1137. DOI: 10.1111/jfd.12443

Eaglesham JB, Pan Y, Kupper TS, and Kranzusch PJ. 2019. Viral and metazoan poxins are cGAMP-specific nucleases that restrict cGAS-STING signalling. Nature, 566(7743): 259–263. DOI: 10.1038/s41586-019-0928-6

Fang Z, and Rajewsky N. 2011. The impact of miRNA target sites in coding sequences and in 3 ′UTRs. PLoS One, 6(3): e18067. DOI: 10.1371/journal.pone.0018067

Friedländer MR, Mackowiak SD, Li N, Chen W, and Rajewsky N. 2012. miRDeep2 accurately identifies known and hundreds of novel microRNA genes in seven animal clades. Nucleic Acids Research, 40(1): 37–52. PMID: 21911355 DOI: 10.1093/nar/gkr688

Gendrault JL, Steffan AM, Bingen A, and Kirn A. 1981. Penetration and uncoating of frog virus 3 (FV3) in cultured rat Kupffer cells. Virology, 112(2): 375–384. DOI: 10.1016/0042-6822(81)90284-1

Goorha R, Murti G, Granoff A, and Tirey R. 1978. Macromolecular synthesis in cells infected by frog virus — VIII. The nucleus is a site of frog virus 3 DNA and RNA synthesis. Virology, 84(1): 32–50. DOI: 10.1016/0042-6822(78)90216-7

Grayfer L, Edholm E, De Jesús Andino F, Chinchar VG, and Robert J. 2015. Ranavirus host immunity and immune rvasion. *In* Ranaviruses. *Edited by* M. Gray and V. Chinchar, Springer, Cham.

Grinberg M, Gilad S, Meiri E, Levy A, Isakov O, Ronen R, et al. 2012. Vaccinia virus infection suppresses the cell microRNA machinery. Archives of Virology, 157(9): 1719–1727. DOI: 10.1007/s00705-012-1366-z

Ho BC, Yang PC, and Yu SL. 2016. MicroRNA and pathogenesis of enterovirus infection. Viruses, 8(1): 11. PMID: 26751468 DOI: 10.3390/v8010011

Honda K, Takaoka A, and Taniguchi T. 2006. Type I interferon [corrected] gene induction by the interferon regulatory factor family of transcription factors. Immunity, 25(3): 349–360. DOI: 10.1016/j.immuni.2006.08.009

Hou J, Wang P, Lin L, Liu X, Ma F, An H, et al. 2009. MicroRNA-146a feedback inhibits RIG-I-dependent Type I IFN production in macrophages by targeting TRAF6, IRAK1, and IRAK2. Journal of Immunology, 183(3): 2150–2158. DOI: 10.4049/jimmunol.0900707

Houts GE, Gravell M, and Granoff A. 1974. Electron microscopic observations on early events of frog virus 3 replication. Virology, 58(2): 589–594. DOI: 10.1016/0042-6822(74)90093-2

Imaizumi T, Tanaka H, Tajima A, Yokono Y, Matsumiya T, Yoshida H, et al. 2010. IFN-gamma and TNF-alpha synergistically induce microRNA-155 which regulates TAB2/IP-10 expression in human mesangial cells. American Journal of Nephrology, 32(5): 462–468. DOI: 10.1159/000321365

InvivoGen Type I IFN Production and Signaling. [online]: Available from invivogen.com.

Jarret A, McFarland AP, Horner SM, Kell A, Schwerk J, Hong M, et al. 2016. Hepatitis-C-virus-induced microRNAs dampen interferon-mediated antiviral signaling. Nature Medicine, 22(12): 1475–1481. DOI: 10.1038/nm.4211

Kärber G. 1931. Beitrag zur kollektiven Behandlung pharmakologischer Reihenversuche. Archiv für experimentelle Pathologie und Pharmakologie, 162: 4. DOI: 10.1007/BF01863914

Karimi K, Fortriede JD, Lotay VS, Burns KA, Wang DZ, Fisher ME, et al. 2018. Xenbase: A genomic, epigenomic and transcriptomic model organism database. Nucleic Acids Research, 46(D1): D861–D868. DOI: 10.1093/nar/gkx936

Kelly DC. 1975. Frog virus 3 replication: electron microscope observations on the sequence of infection in chick embryo fibroblasts. Journal of General Virology, 26(1): 71–86. DOI: 10.1099/0022-1317-26-1-71

Knudson DL, and Tinsley TW. 1974. Replication of a nuclear polyhedrosis virus in a continuous cell culture of *Spodoptera frugiperda*: purification, assay of infectivity, and growth characteristics of the virus. Journal of Virology, 14(4): 934–944. DOI: 10.1128/JVI.14.4.934-944.1974

Kozomara A, Birgaoanu M, and Griffiths-Jones S. 2019. miRBase: from microRNA sequences to function. Nucleic Acids Research, 47(D1): D155–D162. PMID: 30423142 DOI: 10.1093/nar/gky1141

Langmead B, and Salzberg SL. 2012. Fast gapped-read alignment with Bowtie 2. Nature Methods, 9(4): 357–359. DOI: 10.1038/nmeth.1923

Law CW, Alhamdoosh M, Su S, Dong X, Tian L, Smyth GK, et al. 2016. RNA-seq analysis is easy as 1-2-3 with limma, Glimma and edgeR. F1000Research, 5:1408. DOI: 10.12688/f1000research.9005.3

Lee I, Ajay SS, Yook JI, Kim HS, Hong SH, Kim NH, et al. 2009. New class of microRNA targets containing simultaneous 5'-UTR and 3'-UTR interaction sites. Genome Research, 19(7): 1175–1183. DOI: 10.1101/gr.089367.108

Lee Y, Jeon K, Lee JT, Kim S, and Kim VN. 2002. MicroRNA maturation: stepwise processing and subcellular localization. EMBO Journal, 21(17): 4663–4670. DOI: 10.1093/emboj/cdf476

Li J, Xie Y, Li L, Li X, Shen L, Gong J, et al. 2020. MicroRNA-30a modulates type I interferon responses to facilitate coxsackievirus B3 replication via targeting tripartite motif protein 25. Frontiers in Immunology, 11: 603437. PMID: 33519812 DOI: 10.3389/fimmu.2020.603437

Li P, Shen M, Gao F, Wu J, Zhang J, Teng F, et al. 2017. An antagomir to microRNA-106b-5p ameliorates cerebral ischemia and reperfusion injury in rats via inhibiting apoptosis and oxidative stress. Molecular Neurobiology, 54(4): 2901–2921. DOI: 10.1007/s12035-016-9842-1

Lorenz R, Bernhart SH, Höner Zu Siederdissen C, Tafer H, Flamm C, Stadler PF, et al. 2011. ViennaRNA package 2.0. Algorithms for Molecular Biology, 6: 26. DOI: 10.1186/1748-7188-6-26

Love MI, Huber W, and Anders S. 2014. Moderated estimation of fold change and dispersion for RNA-seq data with DESeq2. Genome Biology, 15(12): 550. DOI: 10.1186/s13059-014-0550-8

Marie I, Durbin JE, and Levy DE. 1998. Differential viral induction of distinct interferon-alpha genes by positive feedback through interferon regulatory factor-7. EMBO Journal, 17(22): 6660–6669. DOI: 10.1093/emboj/17.22.6660

Martin M. 2011. Cutadapt removes adapter sequences from high-throughput sequencing reads. EMBnet.Journal, 17(1): 10–12. DOI: 10.14806/ej.17.1.200

Matsumoto M, and Seya T. 2008. TLR3: Interferon induction by double-stranded RNA including poly(I:C). Advanced Drug Delivery Reviews, 60(7): 805–812. DOI: 10.1016/j.addr.2007.11.005

Meng Y, Tian H, Hu Q, Liang H, Zeng L, and Xiao H. 2018. MicroRNA repertoire and comparative analysis of Andrias davidianus infected with ranavirus using deep sequencing. Developmental and Comparative Immunology, 85: 108–114. PMID: 29626489 DOI: 10.1016/j.dci.2018.04.002

Mogensen TH. 2009. Pathogen recognition and inflammatory signaling in innate immune defenses. Clinical Microbiology Reviews, 22(2): 240–273, Table of Contents. DOI: 10.1128/CMR.00046-08

Molteni CG, Principi N, and Esposito S. 2014. Reactive oxygen and nitrogen species during viral infections. Free Radical Research, 48(10): 1163–1169. DOI: 10.3109/10715762.2014.945443

Motwani M, Pesiridis S, and Fitzgerald KA. 2019. DNA sensing by the cGAS-STING pathway in health and disease. Nature Reviews Genetics, 20(11): 657–674. DOI: 10.1038/s41576-019-0151-1

O'Connell RM, Taganov KD, Boldin MP, Cheng G, and Baltimore D. 2007. MicroRNA-155 is induced during the macrophage inflammatory response. Proceedings of the National Academy of Science USA, 104(5): 1604–1609. DOI: 10.1073/pnas.0610731104

Pedersen IM, and Zisoulis DG. 2016. Transposable elements and miRNA: Regulation of genomic stability and plasticity. Mobile Genetic Elements, 6(3): e1175537. DOI: 10.1080/2159256X.2016.1175537

Pham PH, Jung J, and Bols NC. 2011. Using 96-well tissue culture polystyrene plates and a fluorescence plate reader as tools to study the survival and inactivation of viruses on surfaces. Cytotechnology, 63(4): 385–397. DOI: 10.1007/s10616-011-9355-8

Poynter SJ, and DeWitte-Orr SJ. 2015. Length-dependent innate antiviral effects of double-stranded RNA in the rainbow trout (*Oncorhynchus mykiss*) cell line, RTG-2. Fish and Shellfish Immunology, 46(2): 557–565. PMID: 26208750 DOI: 10.1016/j.fsi.2015.07.012

Poynter SJ, and DeWitte-Orr SJ. 2018. Understanding viral dsRNA-mediated innate immune responses at the cellular level using a rainbow trout model. Frontiers in Immunology, 9. DOI: 10.3389/fimmu.2018.00829

Rehmsmeier M, Steffen P, Hochsmann M, and Giegerich R. 2004. Fast and effective prediction of microRNA/target duplexes. RNA, 10(10): 1507–1517. DOI: 10.1261/rna.5248604

Rice P, Longden I, and Bleasby A. 2000. EMBOSS: The European molecular biology open software suite. Trends in Genetics, 16(6): 276–277. DOI: 10.1016/s0168-9525(00)02024-2

Robert J, Edholm ES, Jazz S, Odalys TL, and Francisco JA. 2017. *Xenopus*-FV3 host-pathogen interactions and immune evasion. Virology, 511: 309–319. DOI: 10.1016/j.virol.2017.06.005

Robinson MD, McCarthy DJ, and Smyth GK. 2010. edgeR: A Bioconductor package for differential expression analysis of digital gene expression data. Bioinformatics, 26(1): 139–140. PMID: 19910308 DOI: 10.1093/bioinformatics/btp616

Sang Y, Liu Q, Lee J, Ma W, McVey DS, and Blecha F. 2016. Expansion of amphibian intronless interferons revises the paradigm for interferon evolution and functional diversity. Scientific Reports, 6: 29072. PMID: 27356970 DOI: 10.1038/srep29072

Sato M, Hata N, Asagiri M, Nakaya T, Taniguchi T, and Tanaka N. 1998. Positive feedback regulation of type I IFN genes by the IFN-inducible transcription factor IRF-7. FEBS Letters, 441(1): 106–110. DOI: 10.1016/s0014-5793(98)01514-2

Shapiro JS, Schmid S, Aguado LC, Sabin LR, Yasunaga A, Shim JV, et al. 2014. Drosha as an interferon-independent antiviral factor. Proceedings of the National Academy of Science USA, 111(19): 7108–7113. DOI: 10.1073/pnas.1319635111

Tai L, Huang CJ, Choo KB, Cheong SK, and Kamarul T. 2020. Oxidative stress down-regulates MiR-20b-5p, MiR-106a-5p and E2F1 expression to suppress the G1/S transition of the cell cycle in multipotent stromal cells. International Journal of Molecular Sciences, 17(4): 457–470. DOI: 10.7150/ijms.38832

Tamassia N, Le Moigne V, Rossato M, Donini M, McCartney S, Calzetti F, et al. 2008. Activation of an immunoregulatory and antiviral gene expression program in poly(I:C)-transfected human neutrophils. Journal of Immunology, 181(9): 6563–6573. DOI: 10.4049/jimmunol.181.9.6563

Tan WG, Barkman TJ, Gregory Chinchar V, and Essani K. 2004. Comparative genomic analyses of frog virus 3, type species of the genus Ranavirus (family *Iridoviridae*). Virology, 323(1): 70–84. DOI: 10.1016/j.virol.2004.02.019

Tang Y, Luo X, Cui H, Ni X, Yuan M, Guo Y, et al. 2009. MicroRNA-146A contributes to abnormal activation of the type I interferon pathway in human lupus by targeting the key signaling proteins. Arthritis & Rheumatology, 60(4): 1065–1075. DOI: 10.1002/art.24436

The Gene Ontology Consortium. 2019. The Gene Ontology Resource: 20 years and still GOing strong. Nucleic Acids Research, 47(D1): D330–D338. DOI: 10.1093/nar/gky1055

Tili E, Michaille JJ, Cimino A, Costinean S, Dumitru CD, Adair B, et al. 2007. Modulation of miR-155 and miR-125b levels following lipopolysaccharide/TNF-alpha stimulation and their possible roles in regulating the response to endotoxin shock. Journal of Immunology, 179(8): 5082–5089. DOI: 10.4049/jimmunol.179.8.5082

Varga JFA, Bui-Marinos MP, and Katzenback BA. 2019. Frog skin innate immune defences: sensing and surviving pathogens. Frontiers in Immunology, 9: 3128. PMID: 30692997 DOI: 10.3389/fimmu.2018.03128

Vo NTK, Guerreiro M, Yaparla A, Grayfer L, and DeWitte-Orr SJ. 2019. Class A scavenger receptors are used by Frog virus 3 during its cellular entry. Viruses, 11(2). DOI: 10.3390/v11020093

Wang L, Qin Y, Tong L, Wu S, Wang Q, Jiao Q, et al. 2012. MiR-342-5p suppresses coxsackievirus B3 biosynthesis by targeting the 2C-coding region. Antiviral Research, 93(2): 270–279. DOI: 10.1016/j.antiviral.2011.12.004

Wang L, Wang JK, Han LX, Zhuo JS, Du X, Liu D, et al. 2017. Characterization of miRNAs involved in response to poly(I:C) in porcine airway epithelial cells. Animal Genetics, 48(2): 182–190. DOI: 10.1111/age.12524

Wendel ES, Yaparla A, Melnyk MLS, Koubourli DV, and Grayfer L. 2018. Amphibian (*Xenopus laevis*) tadpoles and adult frogs differ in their use of expanded repertoires of type I and type III interferon cytokines. Viruses, 10(7): 372. DOI: 10.3390/v10070372

Wendlandt EB, Graff JW, Gioannini TL, McCaffrey AP, and Wilson ME. 2012. The role of microRNAs miR-200b and miR-200c in TLR4 signaling and NF-kappaB activation. Innate Immunology, 18(6): 846–855. DOI: 10.1177/1753425912443903

Whitley DS, Yu K, Sample RC, Sinning A, Henegar J, Norcross E, et al. 2010. Frog virus 3 ORF 53R, a putative myristoylated membrane protein, is essential for virus replication in vitro. Virology, 405(2): 448–456. DOI: 10.1016/j.virol.2010.06.034

Witteveldt J, Ivens A, and Macias S. 2018. Inhibition of microprocessor function during the activation of the type I interferon response. Cell Reports, 23(11): 3275–3285. DOI: 10.1016/j.celrep.2018.05.049

Wu J, Ji Z, Qiao M, Peng X, Wu H, Song Z, et al. 2019. MicroRNA transcriptome analysis of poly I:C-stimulated and PRRSV-infected porcine alveolar macrophages. Journal of Applied Genetics, 60(3–4): 375–383. DOI: 10.1007/s13353-019-00500-3

Wu JY, and Kuo CC. 2012. Pivotal role of ADP-ribosylation factor 6 in Toll-like receptor 9-mediated immune signaling. Journal of Biological Chemistry, 287(6): 4323–4334. DOI: 10.1074/jbc.M111.295113

Yang JS, Phillips MD, Betel D, Mu P, Ventura A, Siepel AC, et al. 2011. Widespread regulatory activity of vertebrate microRNA* species. RNA, 17(2): 312–326. DOI: 10.1261/rna.2537911

Zheng Z, Ke X, Wang M, He S, Li Q, Zheng C, et al. 2013. Human microRNA hsa-miR-296-5p suppresses enterovirus 71 replication by targeting the viral genome. Journal of Virology, 87(10): 5645–5656. DOI: 10.1128/JVI.02655-12